Title
Ap4A Regulates Directional Mobility and Antigen Presentation in Dendritic Cells

Authors
La Shu, Shin
Paruchuru, Lakshmi Bhargavi
Tay, Neil Quanwei
et al.

Publication Date
2019-06-01

DOI
10.1016/j.isci.2019.05.045

Peer reviewed

iScience

CellPress

Article

Ap_4A Regulates Directional Mobility and Antigen Presentation in Dendritic Cells

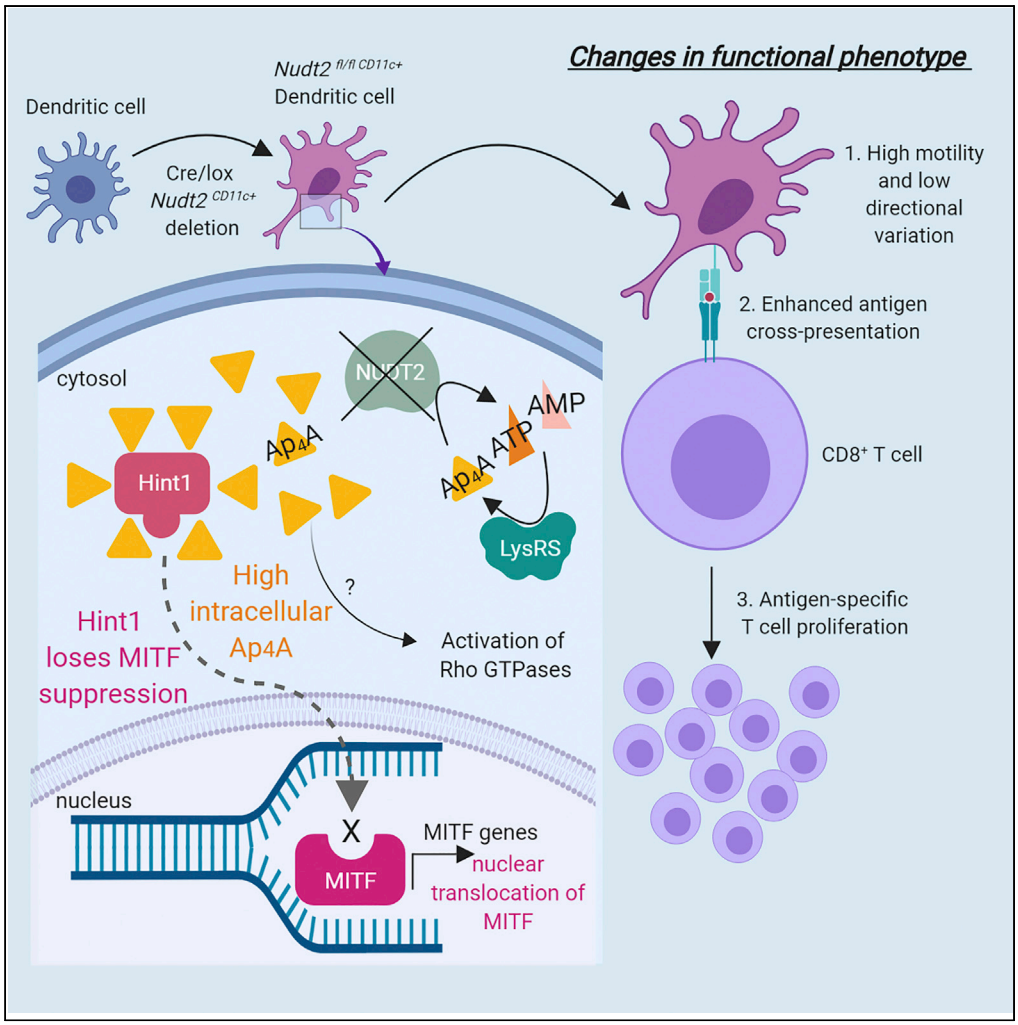

Shin La Shu, Lakshmi Bhargavi Paruchuru, Neil Quanwei Tay, ..., Hovav Nechushtan, Ehud Razin, David Michael Kemeny

hovavnech@hadassah.org.il (H.N.)
ehudr@ekmd.huji.ac.il (E.R.)
mickdm@nus.edu.sg (D.M.K.)

HIGHLIGHTS

DCs of *Nudt2*$^{fl/fl}$/CD11c-cre mice exhibit low directional variability and high motility

DCs elevate proliferation of OVA-specific T cell receptor transgenic CD8$^+$ T cells

The escalation of Ap_4A levels in DCs could enhance their immune protective activity

Mice can serve as useful functional tool to study the role of Ap_4A in various cells

La Shu et al., iScience *16*, 524–534
June 28, 2019
https://doi.org/10.1016/j.isci.2019.05.045

iScience

CellPress

Article

Ap_4A Regulates Directional Mobility and Antigen Presentation in Dendritic Cells

Shin La Shu,[1,2] Lakshmi Bhargavi Paruchuru,[3] Neil Quanwei Tay,[1,2] Yen Leong Chua,[1] Adeline Shen Yun Foo,[2] Chris Maolin Yang,[1,2] Ka Hang Liong,[1,2] Esther Geok Liang Koh,[1,2] Angeline Lee,[1,2] Hovav Nechushtan,[4,*] Ehud Razin,[2,3,5,*] and David Michael Kemeny[1,2,*]

SUMMARY

The significance of intracellular Ap_4A levels over immune activity of dendritic cells (DCs) has been studied in *Nudt2*$^{fl/fl}$/CD11c-cre mice. The transgenic mice have been generated by crossing floxed NUDT2 gene mice with DC marker CD11c recombinase (cre) mice. The DCs derived from these mice have higher levels of Ap_4A (≈30-fold) compared with those derived from *Nudt2*$^{+/+}$ mice. Interestingly, the elevated Ap_4A in DCs has led them to possess higher motility and lower directional variability. In addition, the DCs are able to enhance immune protection indicated by the higher cross-presentation of antigen and priming of CD8$^+$ OT-I T cells. Overall, the study denotes prominent impact of Ap_4A over the functionality of DCs. The *Nudt2*$^{fl/fl}$/CD11c-cre mice could serve as a useful tool to study the influence of Ap_4A in the critical immune mechanisms of DCs.

INTRODUCTION

Transfer ribonucleic acid (tRNA) synthetases play an important role in the central dogma of molecular biology. The specific function of tRNA synthetases is to conjugate tRNAs with the cognate amino acid for correct translation of polypeptides from mRNA. Progressively, highly conserved and non-canonical activities of tRNA synthetases that are unique for each amino acid-charging tRNA synthetase have been discovered. Lysyl-tRNA synthetase (LysRS), a tRNA that charges lysine onto lysine-tRNA for use in ribosome for translation, have also been serving an evolutionarily conserved, non-canonical enzymatic activity to produce diadenosine tetraphosphate (Ap_4A), a small signaling molecule composed of two adenosine moieties joined through a 5′-5′ linkage by a chain of four phosphates. This non-canonical pathway in LysRS is triggered by the phosphorylation of LysRS on serine 207 (P-s207 LysRS) via p38 mitogen-activated protein kinase activity. Phosphorylation leads to the dissociation of P-s207 LysRS from multi-synthetase complex (MSC) and promotes the production of Ap_4A (Ofir-Birin et al., 2013). In turn, the synthesis of Ap_4A is regulated by the housekeeping protein Ap_4A hydrolase (Ap_4AHy) that converts Ap_4A back into its original building blocks (one molecule of ATP and one molecule of AMP) thereby creating a regulatory feedback to maintain intracellular Ap_4A levels (Vollmayer et al., 2003).

Ap_4A synthesis activity by LysRS can directly control specific response programming in immune-specialized cells (Nechushtan et al., 2009). Our group has previously demonstrated that non-canonical LysRS activity can drive increased intracellular Ap_4A and control USF2 transcriptional activity, which up-regulates transforming growth factor-β2 in FcepsilonRI-activated mast cells (Lee and Razin, 2005). Ap_4A can enhance phorbol myristate acetate (PMA)-stimulated reactive oxygen species production in lymphocytes (Schepers et al., 2010) and has been implicated in key immunological responses (Carracedo et al., 2013; Castany et al., 2011; Chang et al., 2014; Louie et al., 1988). Another pathway that is driven by the increase of intracellular Ap_4A is the activation of microphthalmia-associated transcription factor (MITF), a master regulator in melanocyte development (Levy et al., 2006). Hint1, a co-suppressor of MITF, is also inactivated by high intracellular concentration of Ap_4A and dissociates from Hint1. Released MITF can translocate to the nucleus and initiate transcription of downstream genes (Lee et al., 2004a).

Ap_4A is also implicated in the control of antigen presentation. Low levels of Ap_4A are observed in patients with Chediak-Higashi syndrome (Kim et al., 1985), where delayed major histocompatibility complex (MHC) class II-restricted antigen presentation increases pathogen load (Martin-Fernández et al., 2005). The expression of MHC class II is a defining feature of antigen-presenting cells (APCs). Among APCs, dendritic cells (DCs) possess vastly efficient antigen cross-presentation response over all other known immune cell types. DCs possess high motility to bring sampled antigens to naive T cells located in lymph nodes to

[1]Immunology Programme, Department of Microbiology, Centre for Life Sciences, National University of Singapore, #03-09, 28 Medical Drive, Singapore 117456, Singapore

[2]NUS-HUJ-CREATE, 1 Create Way, Innovation Wing #03-09, Singapore 138602, Singapore

[3]Department of Biochemistry and Molecular Biology, Institute for Medical Research Israel-Canada, Hebrew University of Jerusalem, Jerusalem 91120, Israel

[4]Sharett Institute of Oncology, Hadassah Hebrew University Medical Center, Hebrew University of Jerusalem, POB 12000 Jerusalem, Israel

[5]Lead Contact

*Correspondence: hovavnech@hadassah.org.il (H.N.), ehudr@ekmd.huji.ac.il (E.R.), mickdm@nus.edu.sg (D.M.K.)

https://doi.org/10.1016/j.isci.2019.05.045

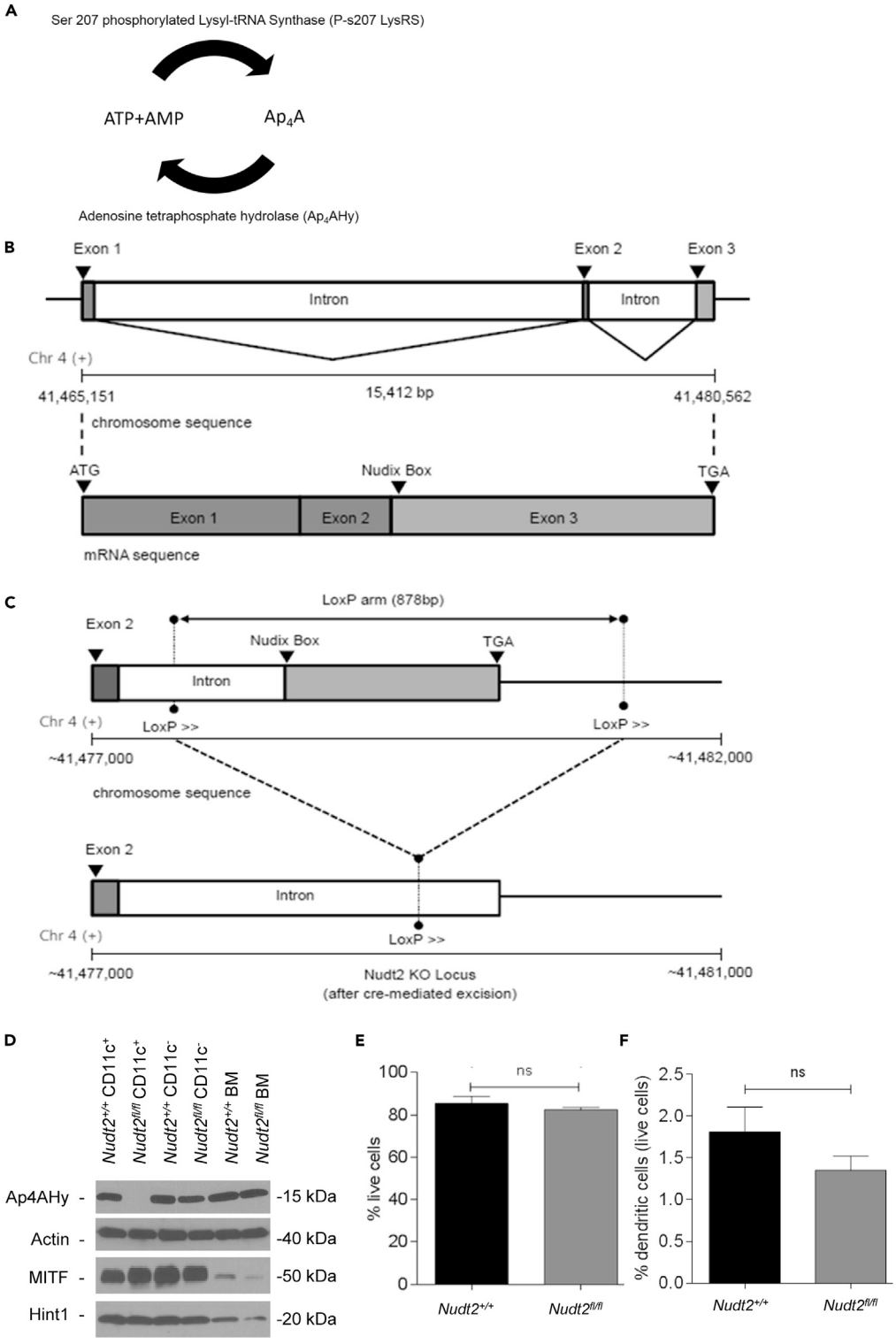

Figure 1. Generation of Ap_4A Hydrolase Knockout Mice and Viability of Dendritic Cells

(A) The phosphorylated form of Lysyl-tRNA transferase (phosphoSerine 207 LysRS) synthesizes Ap_4A from ATP and AMP, and is in turn broken down into same by Ap_4A hydrolase (Ap_4AHy).

Figure 1. *Continued*

(B) The gene locus and mRNA structure of NUDT2. The full open reading frame for Ap_4AHy (15,412 bp) consists of three exons interspersed with two introns. The Nudix box is nothing but the enzymatically functional site for Ap_4AHy and is located at exon 3.

(C) The deletion of $Ap4_AHy$ by gene floxing and deletion strategy. The two *loxP* sites were generated on either side of the gene encompassing the full sequence of exon 3 and a portion of immediate intron upstream to it.

(D–F) (D) Western blot showing expression levels of $Ap4_AHy$, MITF, and Hint1 in splenic dendritic cells of $Nudt2^{+/+}$ and $Nudt2^{fl/fl}$/$CD11c^+$ (Ap_4A hydrolase knockout) mice (represents four independent experiments). Immature bone marrow-derived cells (BM). (E) and (F) Viability percentage of isolated BMDCs and splenic DCs. Results (mean ± SEM) represent two independent experiments. The significant difference of test in comparision to control. $^{ns}p > 0.05$ (Student's t test).

stimulate adaptive immune response. Hence DCs act as connecting linkers between innate and acquired immunity. Immature DCs, although present in blood, are more prevalent in pathogen-prone peripheral tissues. Mature DCs travel toward lymph nodes for the antigen presentation to T and B cells, thus activating acquired immune response (Clark et al., 2000). Harnessing the ability of DC as a professional APC to enhance antigen-specific T cell immune response with high precision is particularly useful for the development of more effective cancer immunotherapy vaccines (Zamarin and Postow, 2015).

DCs adopt a dynamic behavior by migrating to lymph nodes for naive T or B cell priming and maintaining acquired immune activity (Germain et al., 2012). Hence migratory ability of DC is directly correlated with its ability to stimulate immune response through antigen presentation to naive T and B cells in remotely accessible regions of lymph nodes awaiting stimulation by DCs.

We reasoned that if a highly conserved function of APCs such as antigen presentation can be precisely impaired by low levels of intracellular Ap_4A, APCs may functionally benefit from the increase of intracellular Ap_4A concentration. We hypothesized that Ap_4A is able to enhance functional capacities of APCs by improving either mobility or antigen presentation, or both.

The NUDT2 gene encodes Ap_4A hydrolase, a member of the nudix-type family of enzymes that hydrolyze a wide range of pyrophosphates. $CD11c^+$ is preferentially expressed in murine DCs. Ap_4A hydrolase allele was floxed and crossed with a $CD11c^+$ promoter-specific Cre mice to generate the deletion of NUDT2 gene in $CD11c^+$ cells ($Nudt2^{fl/fl}$/CD11c-cre mice). The present study is aimed at investigating the immune modulatory effect of Ap_4A in DCs from $Nudt2^{fl/fl}$/CD11c-cre mice. We report the influence of Ap_4A levels over DCs' viability, motility, and expression of immune activation markers.

RESULTS

Selective Knockout of Ap_4A Hydrolase in Dendritic Cells of $Nudt2^{fl/fl}$/$CD11c^+$ Mice

The intracellular level of Ap_4A is regulated by two enzymes: lysyl tRNA synthetase (LysRS) and Ap_4A hydrolase (Ap_4AHy; Figure 1A). To investigate the function of Ap_4A in DCs, we have utilized a floxed Ap_4A hydrolase allele mouse ($Nudt2^{fl/fl}$; Figure 1B), which we crossed with $CD11c^+$ transgenic mice thereby targeting deletion of Ap_4A hydrolase to cells that expresses the transmembrane surface protein CD11c, i.e., DCs (Figure 1C). The western blot of splenic DC extracts of the mice showed neither any detectable expression of Ap_4AHy nor any disruption in the expression of MITF and Hint1 in $Nudt2^{fl/fl}$/$CD11c^+$ cells when compared with $Nudt2^{+/+}$ $CD11c^+$ cells, confirming successful knockout of Ap_4A hydrolase in DCs of $Nudt2^{fl/fl}$/$CD11c^+$ mice (Figure 1D).

Based on the increased cellular permeability and binding ability with free amines retained in dead cells than live cells, saturation of cells with amines conjugated to florescent APC-Cy7 probe were measured by using flow cytometry to determine the live and dead cell population percentages. The study has revealed a slight decrease in viability of bone marrow DCs (BMDCs) as well as splenic DCs in case of $Nudt2^{fl/fl}$/$CD11c^+$ mice when compared with $Nudt2^{+/+}$ mice and is found to be statistically insignificant (Figures 1E and 1F).

Characterization of Ap_4AHy $Nudt2^{fl/fl}$/$CD11c^+$ DCs

Higher Accumulation of Ap_4A Is Observed in $Nudt2^{fl/fl}$/$CD11c^+$DCs

The intracellular Ap_4A level of BMDCs generated from $Nudt2^{fl/fl}$/$CD11c^+$ and $Nudt2^{+/+}$ mice was examined using a diadenosine nucleotide assay. Compared with $Nudt2^{+/+}$ $CD11c^+$ mice, the BMDCs of $Nudt2^{fl/fl}$/$CD11c^+$ mice contained prominently higher levels of Ap_4A on their third and sixth days of culture

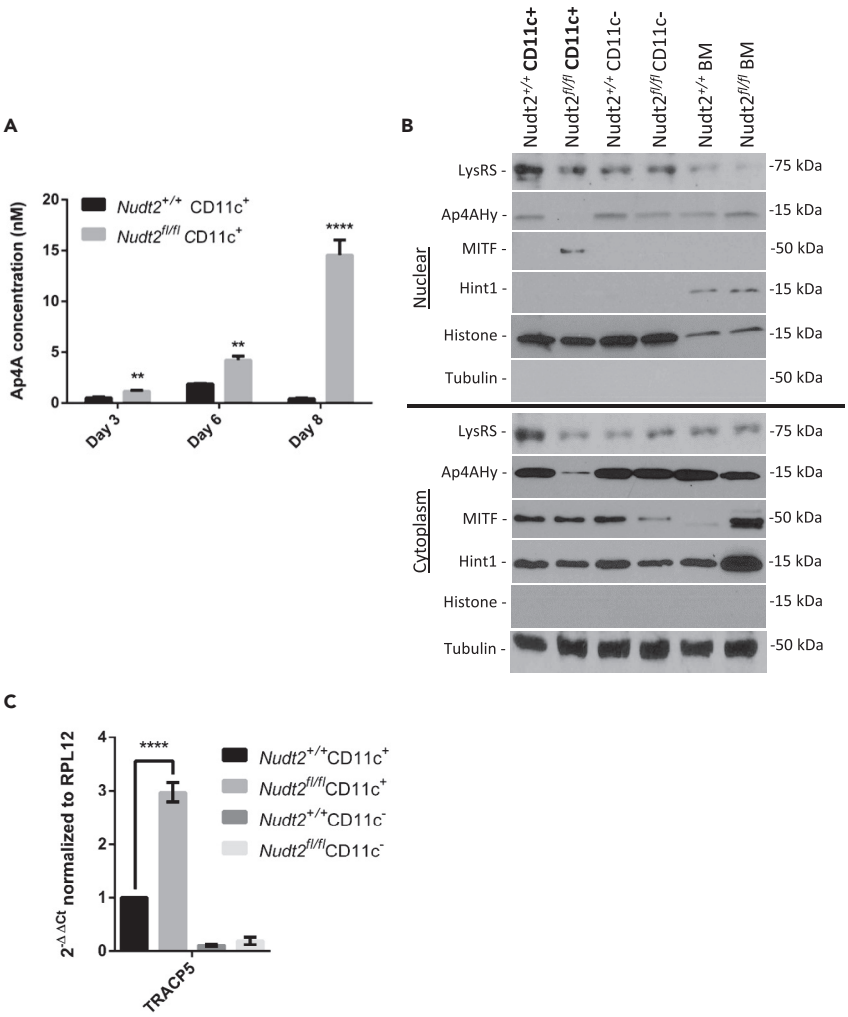

Figure 2. Detailed Functional Characterization of *Nudt2*$^{fl/fl}$/CD11c-cre DC

(A) Intracellular concentrations of Ap_4A in *Nudt2*$^{+/+}$ and *Nudt2*$^{fl/fl}$/CD11c-cre BMDC were generated from bone marrow cultured with granulocyte-macrophage colony-stimulating factor and examined on days 3, 6, and 8, using a luciferase assay.

(B and C) (B) Western blot of LysRS, Ap_4AHy, MITF, and Hint1 in *Nudt2*$^{+/+}$ and *Nudt2*$^{fl/fl}$/CD11c-cre CD11c$^+$ splenic cells. Immature bone marrow-derived cells (BM) (C). Real-time PCR result of MITF-specific gene (TRACP5) expression in BMDCs. The results (mean ± SEM) are representative of four independent experiments and the significant difference of test in comparison to control. **$p < 0.01$; ****$p < 0.0001$ (Mann-Whitney test for multiple comparison).

(2.3- and 3.2-folds, respectively), whereas the levels reached peak state on eighth day of culture (approximately 32-fold; Figure 2A).

Another correlative activation from the increase in intracellular Ap_4A concentration is the initiation of LysRS-Ap_4A-Hint1-MITF pathway. The MITF nuclear localization was examined in splenic DCs and was detected prominently (without concomitant increase in expression) in splenic *Nudt2*$^{fl/fl}$/CD11c$^+$ cells, but not in *Nudt2*$^{+/+}$ CD11c$^+$ cells (Figure 2B). Furthermore, Hint1, a suppressor of MITF, is not present in the nucleus of matured DCs and monocytes and is only present in unmatured BM cells. Hint1 translocation also posits that MITF suppression is released from increased Ap_4A concentration within *Nudt2*$^{fl/fl}$/CD11c$^+$ splenic cells.

To validate the translocation of MITF in to nucleus, which leads to gene transcription, MITF-specific gene tartrate-resistant acid phosphatase 5 (TRACP5) was examined for expression (Luchin et al., 2010). TRACP5 is strongly expressed in both Nudt2$^{+/+}$ and Nudt2$^{fl/fl}$ CD11c$^+$ cells and is upregulated by 2.97-fold in Nudt2$^{fl/fl}$/CD11c$^+$ cells compared with Nudt2$^+$/$^+$ CD11c$^+$ cells (Figure 2C).

To review the association of MITF with LysRS, which occurs during activation of MITF, a pull-down of MITF using LysRS antibody via co-immunoprecipitation experiment was performed on BMDCs. MITF is co-immunoprecipitated using LysRS antibody pull-down in both Nudt2$^{+/+}$ and Nudt2$^{fl/fl}$ DCs, indicating the that binding of LysRS to MITF occurs at baseline level in DCs and the association is increased in Nudt2$^{fl/fl}$ DCs (Figure S1).

Nudt2$^{fl/fl}$/CD11c^{+} BMDCs Possess Greater Motility with Lower Directional Variation

The *Nudt2$^{fl/fl}$*/CD11c^{+} BMDCs have shown vigorous motility as indicated by higher values of distance, speed and displacement compared with *Nudt2$^{+/+}$* BMDCs (Figures 3A–3D). Less directional variability indicates enhanced organization of cytoskeletal dynamics, and such organization generally requires the activation of small GTPases, such as Rho GTPases. The Rho GTPases play a crucial role in cellular migration, of which Rho, Rac, and Cdc42 are widely studied proteins and are highly conserved among eukaryotes (Ridley, 2015). To examine a possible relationship between intracellular Ap_4A increase in DCs and small GTPase activation, active Rac1, cdc42, and RhoA levels were measured (GTP-bound form). The results show a significant decrease in active Rac1 and cdc42, and an increase in RhoA activation levels in case of BMDCs of *Nudt2$^{fl/fl}$*/CD11c^{+} mice compared with that of *Nudt2$^{+/+}$* CD11c^{+} mice (Figure 3E).

Nudt2$^{fl/fl}$/CD11c^{+} DCs Possess Higher Antigen-Presenting and CD8^{+} T Cell-Priming Potential

The possibility of NUDT2 gene directly controlling fundamental immune activity of DCs was also investigated. It is equally important to know whether Nudt2 is important for DC maturation because its status directly impacts the immune function as APCs. Although DCs are highly specialized immune cells that specialize as APCs, they are initially phagocytic before maturation. A change in phagocytic potential would indicate aberrant DC maturation signaling compared with *Nudt2$^{+/+}$* DCs. To measure the phagocytic potential, uptake of fluorescein isothiocyanate (FITC) dextran by DCs was measured. The phagocytic potential of DCs of *Nudt2$^{fl/fl}$*/CD11c^{+} mice was found to be unchanged when compared with that of *Nudt2$^{+/+}$* DCs as the uptake of FITC dextran DCs from *Nudt2$^{fl/fl}$*/CD11c + mice was identical to *Nudt2$^{+/+}$* DCs both at 4°C and 37°C (Figure S2). Therefore, these DCs do not differ in phagocytic capacity, a defining attribute in DC maturation status, indicating that DC maturation status is identical. To determine if antigen presentation functionality is affected, the capacity of DCs to trigger proliferation in antigen-specific T cells that requires DCs to present highly specific antigens to these T cells to trigger activation and proliferation was also investigated. The cultures of BMDCs from either the *Nudt2$^{fl/fl}$*/CD11c^{+} or the *Nudt2$^{+/+}$*/CD11c^{+} mice incubated with OT-1 T cell were co-incubated with positive control SIINFEKL peptides, and have given a similar extent of stimulation of proliferation of CD8^{+} T cells, indicating an overall lack of involvement in the activation of T cells by DCs, which does not require antigen cross-presentation (Figures 4A and 4B). Remarkably, when cultured with DCs co-incubated either with whole ovalbumin (OVA) or OVA and cytosine-phosphodiester linked guanine ligodeoxynucleotides (CpG ODN), there was an average of 20% and 15% higher stimulus in the proliferation of CD8^{+} T cell population, respectively, by the BMDCs from *Nudt2$^{fl/fl}$*/CD11c^{+} mice compared with the *Nudt2$^{+/+}$* BMDCs. *Nudt2* gene is therefore involved in the control of antigen cross-presentation machinery in DCs.

To determine the involvement of interleukin (IL)-12 p40, which is a DC-specialized T cell activation cytokine that controls enhancement of antigen cross-presentation by *Nudt2$^{fl/fl}$*/CD11c^{+} BMDCs, the cytokine levels were measured by ELISA technique. The results revealed a lack of involvement of IL-12 p40 in enhancing the priming of CD8^{+} T cells by *Nudt2$^{fl/fl}$*/CD11c^{+} BMDCs as there was no observable difference in the levels of IL-12 p40 between *Nudt2$^{fl/fl}$*/CD11c^{+} BMDCs and *Nudt2$^{+/+}$* BMDCs (Figure 4C).

Antigen cross-presentation can also be skewed by the change in expression of TAP proteins required for assembly of short peptides onto MHC-I molecules. The mRNA levels of TAP1, TAP2, and TAPASIN were measured in *Nudt2$^{fl/fl}$*/CD11c^{+} DCs as well as in *Nudt2$^{+/+}$* DCs. The results have shown a lack of difference in TAP1, TAP2, or TAPASIN between *Nudt2$^{fl/fl}$*/CD11c-cre or *Nudt2$^{+/+}$* DCs indicating lack of their involvement (Figure 4D). Taken together, *Nudt2* gene is involved in controlling antigen cross-presentation machinery that directly signals T cell proliferation.

DISCUSSION

This study shows that intracellular Ap_4A can be upregulated in immune cells of a specific lineage (DCs) within an *in vivo* model. The DCs from these mice are lacking Ap_4A hydrolase, and a consequent rise in intracellular Ap_4A amounts is observed, revealing an obvious substantial regulation of Ap_4A

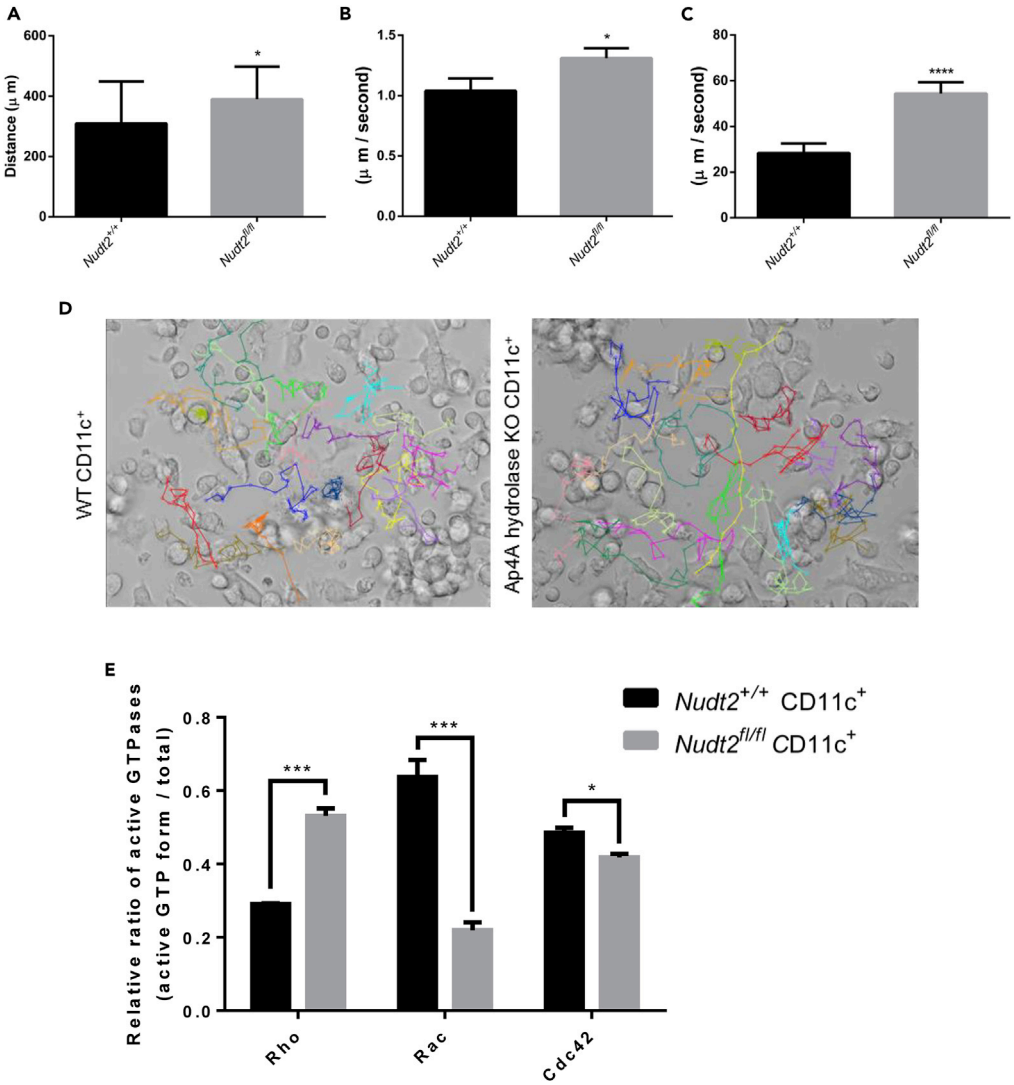

Figure 3. Comparative Motility of DCs from *Nudt2*$^{fl/fl}$/CD11c^{+} and *Nudt2*$^{+/+}$ Mice

(A) Live imaging microscopy of granulocyte-macrophage colony-stimulating factor-treated DCs (8 days). The post-treated DCs on observational Petri dish were chosen randomly (n = 20) and traced minute wise (time lap ≈30 min) to find the change in cell movement and the distance moved.

(B) The speed of cellular movement and the ratio between the distance moved and difference of two time frames.

(C) Cellular displacement.

(D) A still frame taken from the video created for live cell imaging of *Nudt2*$^{+/+}$ and *Nudt2*$^{fl/fl}$/CD11c^{+} DCs.

(E) Small GTPase activation state in *Nudt2*$^{+/+}$ and *Nudt2*$^{fl/fl}$/CD11c^{+} DCs (n = 2). Results (mean ± SEM) represent two independent experiments. The significant difference of test in comparision to control. *$p < 0.05$, ***$p < 0.001$, and ****$p < 0.0001$ (Student's t test or Mann-Whitney test for multiple comparison).

concentrations in DCs by Ap_4A hydrolase through the NUDT2 gene. The *Nudt2*$^{fl/fl}$/CD11c^{+} mice did not exhibit any observable physiological differences to wild-type, leading to the inference that they harbor similar small population of CD11c^{+} cells as are normally present. In addition, their viability remained almost similar.

DCs play a pivotal role in adaptive immunity and tolerance. Efficient migration for accurate positioning to capture antigens from invading pathogens and capacity to process the foreign peptides into recognizable MHC-I-bound complexes through antigen-cross presentation are two immutable purposes of DCs. These functions are therefore critical for immune protection. Most of the immature and highly phagocytic DCs

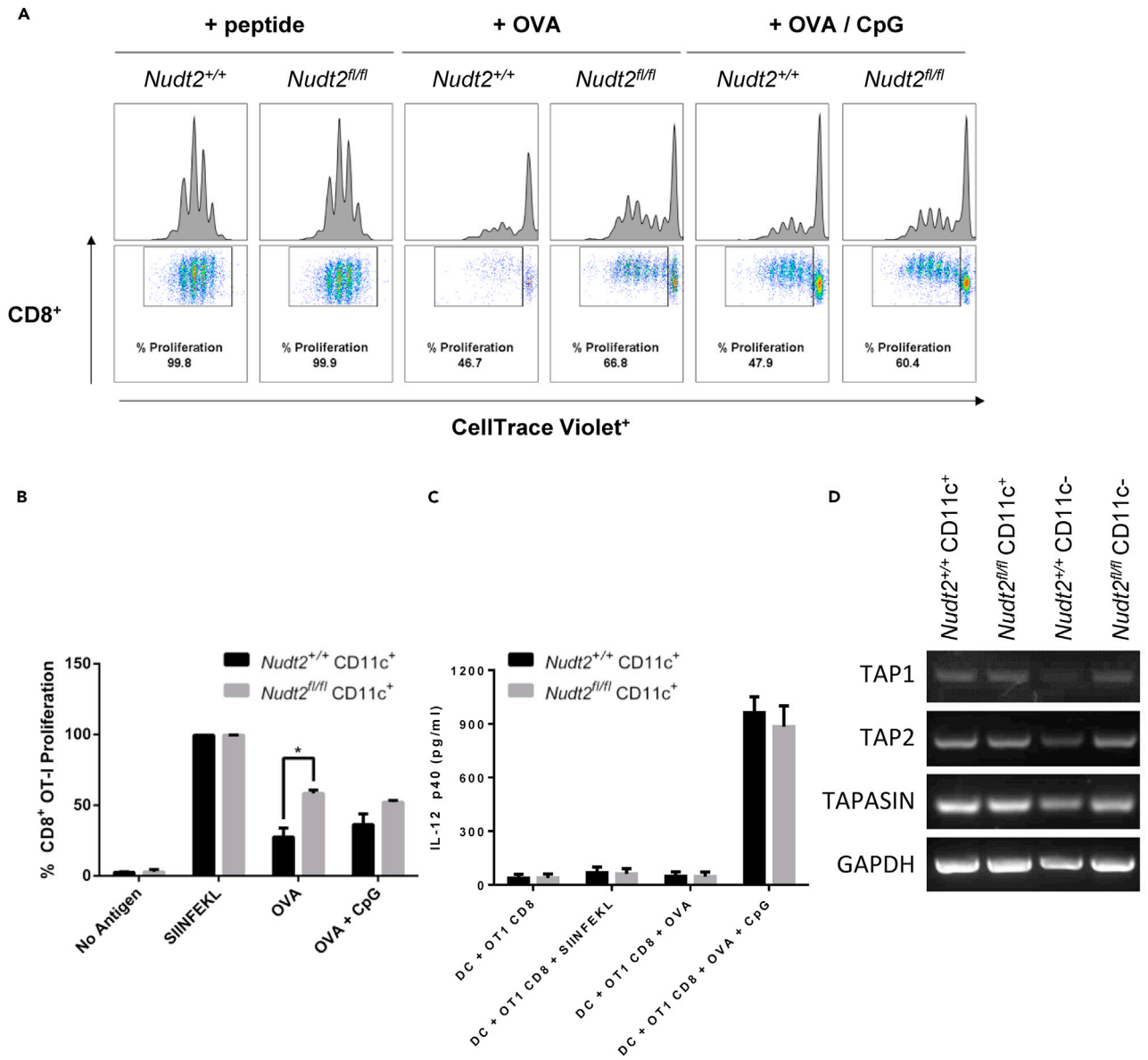

Figure 4. *Nudt2*$^{fl/fl}$/CD11c^{+} DCs' Potential in Influencing OT-I CD8^{+} T Cells Antigen Cross-Priming

(A) The percentage of OT-I CD8^{+} T cells that have proliferated following co-culture for 3 days either with *Nudt2*$^{fl/fl}$/CD11c^{+} BMDCs or *Nudt2*$^{+/+}$ CD11c^{+} BMDCs (1:10) incubated with SIINFEKL peptide, OVA and CpG ODN. The harvested cells were analyzed by flow cytometry to quantify CD8^{+} CellTrace Violet^{+} population for proliferation.

(B) Graph represents the percentage of OT-I CD8^{+} T cells proliferated when cultured with *Nudt2*$^{+/+}$ or *Nudt2*$^{fl/fl}$/CD11c^{+} DCs in response to different antigenic preparations.

(C) IL-12 p40 production by DCs during the above co-culture conditions.

(D) mRNA levels for TAP1, TAP2, and TAPASIN in *Nudt2*$^{+/+}$ and *Nudt2*$^{fl/fl}$/CD11c-cre in splenic DCs measured by RT-PCR. Results (mean ± SEM) represent three independent experiments and the significant difference of test in comparision to control. *$p < 0.05$ (Student's t test or Mann-Whitney test for multiple comparison).

begin their voyage from the bone marrow where they are generated, followed by entry into the blood and sequential movement into peripheral lymphoid tissues (PLTs) and non-lymphoid tissues (NLTs). The DCs possess advanced migratory skills, and their main function in NLTs is the carriage and presentation of antigenic components into and within secondary lymphoid organs (Alvarez et al., 2008). Once primed by the phagocytosis of foreign antigens the enrouted Ag-bearing DCs in lymph nodes begin to build up an immune-stimulatory phenotype, exhibiting increased expression of MHC complexes as well as upregulation

of the co-stimulatory molecules and cytokines required for effective T cell priming. The non-retained DCs enter into the blood stream (blood-borne DCs) and deliver the antigenic components to the spleen (Mullins et al., 2003) and also to PLTs (Cavanagh et al., 2005).

The relationship between *Nudt2* and DC is unknown, but its association with immune function has been speculated. A recent RNA sequencing analysis of *Nudt2* knockout myelogenous leukemia cells revealed that the majority of the target genes are linked to immune-specific processes such as interferon-associated inflammatory responses, MHC-II antigen presentation, allograft rejection, and B cell development (Marriott et al., 2016). The current study focused on the influence of Ap_4A over immune activity of DCs from *Nudt2*$^{fl/fl}$/CD11c^{+} mice and has confirmed that *Nudt2* gene has influence over MHC-II antigen presentation.

Ap_4A regulates MITF activation through the release of Hint1 suppression and consequent nuclear localization of MITF. The nuclear localization of MITF, as a result of increase of Ap_4A, is a hallmark of the LysRS-Ap_4A-Hint1-MITF pathway (Carmi-Levy et al., 2008; 2011; Huete et al., 2011; Lee and Razin, 2005; Lee et al., 2004b; Tshori et al., 2013). The LysRS-Ap_4A-Hint1-MITF pathway has been described in mast cells (Lee et al., 2004a), but it was not clear whether the same pathway is active in DCs.

The LysRS-Ap_4A-Hint1-MITF pathway was examined in DCs in this study, and it was revealed that the increase in MITF nuclear localization, but not HINT-1, in response to the elevated Ap_4A levels is due to the knockout of NUDT2 gene. The binding of MITF to LysRS using co-immunoprecipitation pull down of MITF using LysRS antibody establishes the existence of LysRS-Ap_4A-Hint1-MITF pathway in DCs and further confirms that Hint1 suppression is lifted so that LysRS can bind active MITF.

The BMDCs from *Nudt2*$^{fl/fl}$/CD11c-cre mice cultured from undifferentiated monocytes did not show any morphological or phenotypic differences to *Nudt2*$^{+/+}$ DCs. Interestingly, the DCs of *Nudt2*$^{fl/fl}$/CD11c^{+} mice exhibited a unique pattern of cellular motility with higher velocity and lower directional variability. This suggests that the majority population of DCs of *Nudt2*$^{fl/fl}$/CD11c^{+} mice is having uniform directional imprint that may indicate effective migration toward the immune reaction zones. Furthermore, we found such behavior was correlated to the variation in their expression of small GTPases, i.e., cdc42, Rac1, and RhoA. Our findings provide evidence that reduced activation of Rac1 in DCs leads to increased directional motility, consistent with the earlier studies over fibroblasts that had shown their enhancement of directional motility by the inactivation of the same GTPases (Hanna and El-Sibai, 2013). Among small GTPases that are important in cell motility, Rho GTP is critical for inducing actomyosin contraction and inhibiting actin filament disassembly for cell polarity and directional migration (Kimura et al., 1998; Maekawa et al., 1999). Upregulation of active Rho is observed in CD11c^{+} DC derived from *Nudt2*$^{fl/fl}$ mice. Pharmacologic Rho effector blockades (e.g., ROCK inhibitors) can profoundly decrease DC migration capability. Hence increased bioavailability of RhoGTP can correlate with the increased mobility observed in CD11c^{+} DC derived from *Nudt2*$^{fl/fl}$ mice. Increase in Rho activity also causes decreased availability of Rac (Ohta et al., 2006), and this is likewise also observed in CD11c^{+} DC derived from *Nudt2*$^{fl/fl}$ mice.

The defining feature of DCs is their ability to take up antigen in the periphery, through their dendrites; to withdraw those dendrites; and then to migrate to lymph nodes. Upon regaining their former shapes in lymph node, DCs will present antigenic peptides to CD4^{+} and CD8^{+} T cells. Thus DCs may be regarded as the "shape-shifters" of the immune system. Cross-presentation is the intracellular degradation of extrinsic antigen and its presentation by MHC-I. This important DC function activates CD8^{+} T cells during an immunological response to intracellular pathogens (Murphy and McLennan, 2004; Murphy et al., 2000) and is a highly energy-dependent process and requires movement of the cells into finding suitable T cells. Though identical levels of phagocytic potential, Class-II MHC display and expression of co-stimulatory molecules were seen in DCs of *Nudt2*$^{fl/fl}$/CD11c^{+} mice, there was an enhancement in their immune functionality. These DCs have increased immune activity in terms of antigen processing and cross-presentation in priming the proliferation of CD8^{+} T cells. *In vitro* antigen presentation assay using OT-1 CD8^{+} T cells is well suited to validate this result as an antigen-specific response. The activation of CD8^{+} T cells of OT-1 mice is exclusive for antigen presentation of OVA through DC cross-presentation machinery, and the subsequent trigger of proliferation in OT-1 CD8^{+} T cells is a highly specific response against cross-presented MHC-I antigen on APCs. CD11c^{+} DC derived from *Nudt2*$^{fl/fl}$ mice are capable of

driving the proliferation of antigen-specific $CD8^+$ T cells without the need for CpG ODN, a potent immune agonist (Ramírez-Pineda et al., 2004). However, this observation was found not associated with the expected alteration in the elements of MHC-I machinery, reflecting the possible positive influence of directional motility making effective contact to the T cells and also the rise in the duration of functioning in antigen presentation process. There is direct evidence in support of one of our assumption. Other groups have also reported that overexpression of Rho can directly increase the ability of DC to present OVA peptide to specific T cells (Shurin et al., 2005). Our studies indicate that the increased $CD8^+$ T cell cross-priming potential of DC from *Nudt2*$^{fl/fl}$/$CD11c^+$ mice compared with *Nudt2*$^{+/+}$ is more likely the result of RhoA activation and RAC1 repression. This is in agreement with the earlier studies (Hanna and El-Sibai, 2013; Shurin et al., 2005; Wu et al., 2009).

Another important feature of DCs is their capacity to steer the immune response into clinically beneficial Th1-type immune response by the production of IL-12 (Muller-Berghaus et al., 2005). Without stimulation, IL-12 production is not observed to be different than *Nudt2*$^{+/+}$ for $CD11c^+$ DC derived from *Nudt2*$^{fl/fl}$ mice, indicating that the resultant DCs are not activated immune response without stimuli. Presence of CpG ODN increased IL-12 production but by an identical amount to *Nudt2*$^{+/+}$ mice, suggesting that the $CD11c^+$ DC derived from *Nudt2*$^{fl/fl}$ mice are neither functionally impaired or overactivated compared with *Nudt2*$^{+/+}$ DC counterparts.

In conclusion, increased Ap_4A concentration in DC of *Nudt2*$^{fl/fl}$/$CD11c^+$ mice led to the localization of MITF into the nucleus during restive conditions compared with *Nudt2*$^{+/+}$ DC. These Ap_4A enriched DCs have prominently exhibited alteration in small GTPases rising their motility and antigen presenting potentiality. This study documents an *in vivo* model that can modulate the intracellular Ap_4A concentration by knocking out Ap_4A hydrolase and enhancing antigen cross-presentation by DC. Fundamentally, enhanced antigen cross-presentation in a controlled manner will benefit a wide variety of APC-associated functions such as earlier pathogen recognition by the immune system and better loading and presentation of tumor antigens to cytotoxic $CD8^+$ T cells in response to cancer. The highly specific control of intracellular Ap_4A concentration through manipulation of *NUDT2* gene makes this mechanism an attractive pharmacological target to enhance antigen presentation while keeping the complex repertoire of transcriptional activation of APCs as intact as possible.

Limitations of the Study

The currently studied *Nudt2*$^{fl/fl}$/$CD11c^+$ mice model is an excellent *in vivo* system to understand the consequences of increased intracellular Ap_4A. It is important and yet to be determined whether the circulatory DCs in *Nudt2*$^{fl/fl}$/$CD11c^+$ mice exhibit elevation in antigen presentation to T cells. Also, the identification of key cytokines responsible for DC-specialized T cell activation would become significant. In addition, this study necessitates the elucidation of Ap_4A-binding proteins that are associated with cellular migration in future.

METHODS

All methods can be found in the accompanying Transparent Methods supplemental file.

SUPPLEMENTAL INFORMATION

Supplemental Information can be found online at https://doi.org/10.1016/j.isci.2019.05.045.

ACKNOWLEDGMENTS

The present study was supported in part by grants from the National University of Singapore to D.M.K.; Israel Science Foundation, 115/2013, and Hebrew-University-National Research Foundation of Singapore HUJ-CREATE (R182-005-172-281) to E.R. Graphical abstract was created with bio-render.com.

AUTHOR CONTRIBUTIONS

S.L.S., N.Q.T., A.S.Y.F., K.H.L., E.G.L.K., and A.L. performed the experimental work. Y.L.C. produced the *Nudt2*$^{fl/fl}$/CD11c-cre mice and C.M.Y. designed the experiments. S.L.S. and L.B.P. analyzed the data and drafted the manuscript. D.M.K. and E.R., the principal investigators, conceived the study design and wrote the grant, and with H.N corrected the manuscript. The authors thank Paul Hutchinson and Teoh Guo Hui of

the NUS immunology programme flow cytometry facility for their help and advice on the flow cytometry assays used in this study.

DECLARATION OF INTERESTS

The authors declare no competing interests.

Received: January 10, 2019
Revised: February 25, 2019
Accepted: May 30, 2019
Published: June 28, 2019

REFERENCES

Alvarez, D., Vollmann, E.H., and von Andrian, U.H. (2008). Mechanisms and consequences of dendritic cell migration. Immunity *29*, 325–342.

Carmi-Levy, I., Yannay-Cohen, N., Kay, G., Razin, E., and Nechushtan, H. (2008). Diadenosine tetraphosphate hydrolase is part of the transcriptional regulation network in immunologically activated mast cells. Mol. Cell. Biol. *28*, 5777–5784.

Carmi-Levy, I., Motzik, A., Ofir-Birin, Y., Yagil, Z., Yang, C.M., Kemeny, D.M., Han, J.M., Kim, S., Kay, G., Nechushtan, H., et al. (2011). Importin beta plays an essential role in the regulation of the LysRS-Ap(4)A pathway in immunologically activated mast cells. Mol. Cell. Biol. *31*, 2111–2121.

Carracedo, G., Guzman-Aranguez, A., Loma, P., and Pintor, J. (2013). Diadenosine polyphosphates release by human corneal epithelium. Exp. Eye Res. *113*, 156–161.

Castany, M., Jordi, I., Catala, J., Gual, A., Morales, M., Gasull, X., and Pintor, J. (2011). Glaucoma patients present increased levels of diadenosine tetraphosphate, Ap4A, in the aqueous humour. Exp. Eye Res. *92*, 221–226.

Cavanagh, L.L., Bonasio, R., Mazo, I.B., Halin, C., Cheng, G., van der Velden, A.W.M., Cariappa, A., Chase, C., Russell, P., Starnbach, M.N., et al. (2005). Activation of bone marrow–resident memory T cells by circulating, antigen-bearing dendritic cells. Nat. Immunol. *6*, 1029.

Chang, H., Yanachkov, I.B., Dix, E.J., Yanachkova, M., Li, Y., Barnard, M.R., Wright, G.E., Michelson, A.D., and Frelinger, A.L. (2014). Antiplatelet activity, P2Y1 and P2Y12 inhibition, and metabolism in plasma of stereoisomers of diadenosine 5′,5‴-P1,P4-dithio-P2,P3-chloromethylenetetraphosphate. PLoS One *9*, e94780.

Clark, G.J., Angel, N., Kato, M., López, J.A., MacDonald, K., Vuckovic, S., and Hart, D.N. (2000). The role of dendritic cells in the innate immune system. Microbes Infect. *2*, 257–272.

Germain, R.N., Robey, E.A., and Cahalan, M.D. (2012). A decade of imaging cellular motility and interaction dynamics in the immune system. Science *336*, 1676–1681.

Hanna, S., and El-Sibai, M. (2013). Signaling networks of Rho GTPases in cell motility. Cell. Signal. *25*, 1955–1961.

Huete, F., Guzman-Aranguez, A., Ortin, J., Hoyle, C.H.V., and Pintor, J. (2011). Effects of diadenosine tetraphosphate on FGF9-induced chloride flux changes in achondroplastic chondrocytes. Purinergic Signal. *7*, 243–249.

Kim, B.K., Chao, F.C., Leavitt, R., Fauci, A.S., Meyers, K.M., and Zamecnik, P.C. (1985). Diadenosine 5′,5‴-p1,p4-tetraphosphate deficiency in blood platelets of the Chediak-Higashi syndrome. Blood *66*, 735–737.

Kimura, K., Fukata, Y., Matsuoka, Y., Bennett, V., Matsuura, Y., Okawa, K., Iwamatsu, A., and Kaibuchi, K. (1998). Regulation of the association of adducin with actin filaments by rho-associated kinase (Rho-kinase) and myosin phosphatase. J. Biol. Chem. *273*, 5542–5548.

Lee, Y.-N., and Razin, E. (2005). Nonconventional involvement of LysRS in the molecular mechanism of USF2 transcriptional activity in FcεRI-activated mast cells. Mol. Cell. Biol. *25*, 8904–8912.

Lee, Y.-N., Nechushtan, H., Figov, N., and Razin, E. (2004a). The function of lysyl-tRNA synthetase and Ap4A as signaling regulators of MITF activity in FcepsilonRI-activated mast cells. Immunity *20*, 145–151.

Lee, Y.-N., Nechushtan, H., Figov, N., and Razin, E. (2004b). The function of Lysyl-tRNA synthetase and Ap4A as signaling regulators of MITF activity in FcεRI-activated mast cells. Immunity *20*, 145–151.

Levy, C., Lee, Y.-N., Nechushtan, H., Schueler-Furman, O., Sonnenblick, A., Hacohen, S., and Razin, E. (2006). Identifying a common molecular mechanism for inhibition of MITF and STAT3 by PIAS3. Blood *107*, 2839–2845.

Louie, S., Kim, B.K., and Zamecnik, P. (1988). Diadenosine 5′,5‴-p1,p4 -tetraphosphate, a potential antithrombotic agent. Thromb. Res. *49*, 557–565.

Luchin, A., Purdom, G., Murphy, K., Clark, M.-Y., Angel, N., Cassady, A.I., Hume, D.A., and Ostrowski, M.C. (2010). The microphthalmia transcription factor regulates expression of the tartrate-resistant acid phosphatase gene during terminal differentiation of osteoclasts. J. Bone Miner. Res. *15*, 451–460.

Maekawa, M., Ishizaki, T., Boku, S., Watanabe, N., Fujita, A., Iwamatsu, A., Obinata, T., Ohashi, K., Mizuno, K., and Narumiya, S. (1999). Signaling from Rho to the actin cytoskeleton through protein kinases ROCK and LIM-kinase. Science *285*, 895–898.

Marriott, A.S., Vasieva, O., Fang, Y., Copeland, N.A., McLennan, A.G., and Jones, N.J. (2016). NUDT2 disruption elevates diadenosine tetraphosphate (Ap4A) and down-regulates immune response and cancer promotion genes. PLoS One *11*, e0154674.

Martin-Fernández, J.M., Cabanillas, J.A., Rivero-Carmena, M., Lacasa, E., Pardo, J., Anel, A., Ramirez-Duque, P.R., Merino, F., Rodriguez-Gallego, C., and Regueiro, J.R. (2005). Herpesvirus saimiri-transformed CD8+ T cells as a tool to study Chediak-Higashi syndrome cytolytic lymphocytes. J. Leukoc. Biol. *77*, 661–668.

Muller-Berghaus, J., Olson, W.C., Moulton, R.A., Knapp, W.T., Schadendorf, D., and Storkus, W.J. (2005). IL-12 production by human monocyte-derived dendritic cells. J. Immunother. *28*, 306–313.

Mullins, D.W., Sheasley, S.L., Ream, R.M., Bullock, T.N.J., Fu, Y.-X., and Engelhard, V.H. (2003). Route of immunization with peptide-pulsed dendritic cells controls the distribution of memory and effector T cells in lymphoid tissues and determines the pattern of regional tumor control. J. Exp. Med. *198*, 1023–1034.

Murphy, G.A., and McLennan, A.G. (2004). Synthesis of dinucleoside tetraphosphates in transfected cells by a firefly luciferase reporter gene. Cell. Mol. Life Sci. *61*, 497–501.

Murphy, G.A., Halliday, D., and McLennan, A.G. (2000). The Fhit tumor suppressor protein regulates the intracellular concentration of diadenosine triphosphate but not diadenosine tetraphosphate. Cancer Res. *60*, 2342–2344.

Nechushtan, H., Kim, S., Kay, G., and Razin, E. (2009). Chapter 1: the physiological role of lysyl tRNA synthetase in the immune system. Adv. Immunol. *103*, 1–27.

Ofir-Birin, Y., Fang, P., Bennett, S., Zhang, H.-M., Wang, J., Rachmin, I., Shapiro, R., Song, J., Dagan, A., Pozo, J., et al. (2013). Structural switch of lysyl-tRNA synthetase between translation and transcription. Mol. Cell *49*, 30–42.

Ohta, Y., Hartwig, J.H., and Stossel, T.P. (2006). FilGAP, a Rho- and ROCK-regulated GAP for Rac

binds filamin A to control actin remodelling. Nat. Cell Biol. *8*, 803–814.

Ramírez-Pineda, J.R., Fröhlich, A., Berberich, C., and Moll, H. (2004). Dendritic cells (DC) activated by CpG DNA ex vivo are potent inducers of host resistance to an intracellular pathogen that is independent of IL-12 derived from the immunizing DC. J. Immunol. *172*, 6281–6289.

Ridley, A.J. (2015). Rho GTPase signalling in cell migration. Curr. Opin. Cell Biol. *36*, 103–112.

Schepers, E., Glorieux, G., Jankowski, V., Dhondt, A., Jankowski, J., and Vanholder, R. (2010). Dinucleoside polyphosphates: newly detected uraemic compounds with an impact on leucocyte oxidative burst. Nephrol. Dial. Transplant. *25*, 2636–2644.

Shurin, G.V., Tourkova, I.L., Chatta, G.S., Schmidt, G., Wei, S., Djeu, J.Y., and Shurin, M.R. (2005). Small rho GTPases regulate antigen presentation in dendritic cells. J. Immunol. *174*, 3394–3400.

Tshori, S., Razin, E., and Nechushtan, H. (2013). Amino-acyl tRNA synthetases generate dinucleotide polyphosphates as second messengers: functional implications. Top. Curr. Chem. *344*, 189–206.

Vollmayer, P., Clair, T., Goding, J.W., Sano, K., Servos, J., and Zimmermann, H. (2003). Hydrolysis of diadenosine polyphosphates by nucleotide pyrophosphatases/phosphodiesterases. Eur. J. Biochem. *270*, 2971–2978.

Wu, Y.I., Frey, D., Lungu, O.I., Jaehrig, A., Schlichting, I., Kuhlman, B., and Hahn, K.M. (2009). A genetically encoded photoactivatable Rac controls the motility of living cells. Nature *461*, 104–108.

Zamarin, D., and Postow, M.A. (2015). Immune checkpoint modulation: rational design of combination strategies. Pharmacol. Ther. *150*, 23–32.

ISCI, Volume *16*

Supplemental Information

Ap_4A Regulates Directional Mobility and Antigen Presentation in Dendritic Cells

Shin La Shu, Lakshmi Bhargavi Paruchuru, Neil Quanwei Tay, Yen Leong Chua, Adeline Shen Yun Foo, Chris Maolin Yang, Ka Hang Liong, Esther Geok Liang Koh, Angeline Lee, Hovav Nechushtan, Ehud Razin, and David Michael Kemeny

Supplemental Figure Legends

Figure S1. FITC-dextran phagocytosis assay. *Nudt2*$^{+/+}$ and *Nudt2*$^{fl/fl}$ DCs do not differ in phagocytic capacity, a defining attribute in DC maturation status, indicating that in terms of DC maturation status based on phagocytic capacity they are identical.

Figure S2. MITF association with LysRS. Pull-down of MITF using LysRS antibody in a co-immunoprecipitation experiment was performed in BMDC.

Figure S1.

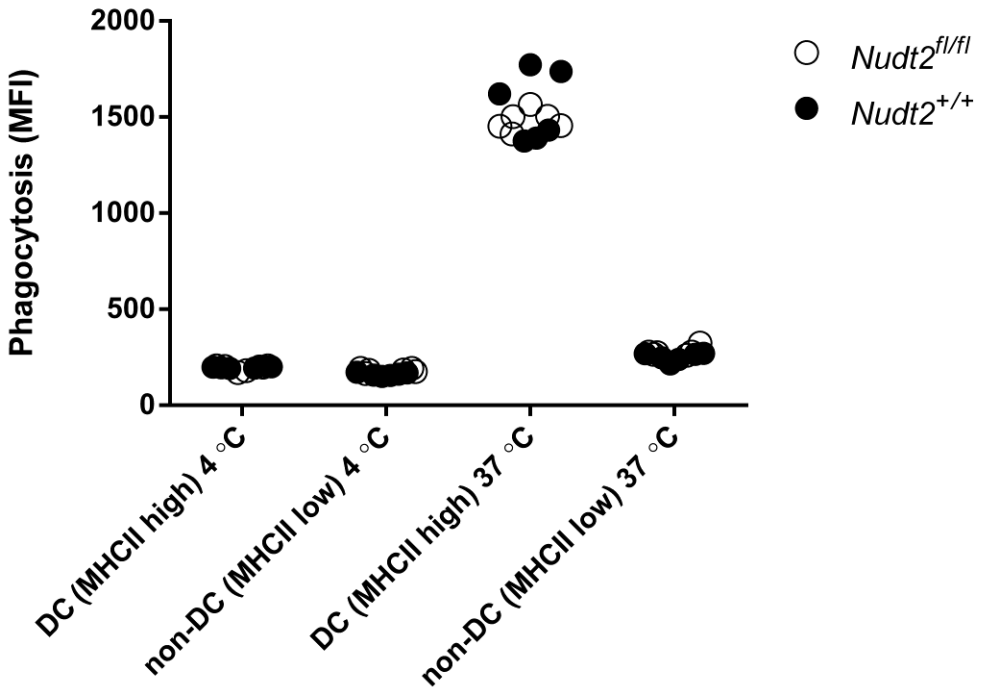
Phagocytosis (MFI)
2000
1500
1000
500
0
DC (MHCII high) 4 ◦C
non-DC (MHCII low) 4 ◦C
DC (MHCII high) 37 ◦C
non-DC (MHCII low) 37 ◦C
Nudt2fl/fl
Nudt2+/+

Figure S2.

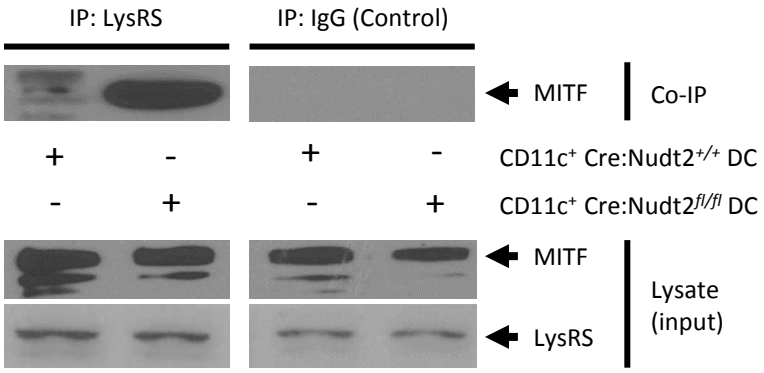
IP: LysRS
IP: IgG (Control)
MITF
Co-IP
+ - + -
CD11c+ Cre:Nudt2+/+ DC
- + - +
CD11c+ Cre:Nudt2fl/fl DC
MITF
LysRS
Lysate
(input)

Transparent Methods

1. Materials and methods

1.1 Mice

The C57BL/6 mice (8-10 weeks old) and OT-1 mice were purchased from National University of Singapore CARE and Charles River Laboratories, respectively, and were bred at NUS CARE. *Nudt2*$^{fl/fl}$ mice were generated by OZ-gene. CD11c-cre transgenic (C57BL/6$^{CD11c\text{-}cre}$) mice were gifted from Florent Ginhoux (SIgN, A*STAR, Singapore). The *Nudt2*$^{fl/fl}$ mice were backcrossed to c57bl/6 mice for nine generations and crossbred with c57bl/6$^{CD11c\text{-}cre}$ for 3 generations to generate *Nudt2*$^{fl/fl}$/CD11c-cre mice. Both age and sex-matched littermate control mice were used in all experiments. All mice were maintained under pathogen-free conditions in the satellite animal house unit. All experiments were performed in accordance with the strict guidelines of the National Advisory Committee for Laboratory Animal Research (NACLAR), Singapore. The Institutional Animal Care and Use Committee of the National University of Singapore have approved the protocols (Protocol number: 102/10).

1.2 Diadenosine nucleotide assay

The nucleotide assay detects the amount of Ap_4A present in extracts of mammalian cells. For each determination, bone marrow cells were seeded at a density of 2 x 10^6 cells per well and cultured for 7 days in accordance to

the method outlined in methods section 1.6 (generation of BMDCs). For the generation of BMDCs, cells in one well of a 6-well plate was grown for 3 to 8 days as specified. The cell layer was washed with warm serum-free medium and lysed with 0.4 M trichloroacetic acid. The extraction cum measurement of the nucleotides using luminometry was performed as described previously (Murphy *et al.*, 2000).

1.3 Quantitative polymerase chain reaction (qPCR)

Total RNA was isolated from sorted splenic DCs using the RNeasy kit (Qiagen, CA, USA), followed by cDNA synthesis using QuantiTect Reverse Transcription kit (Qiagen). Both kits were used according to manufacturer's instructions. Real-time PCR was performed on an ABI7500 real-time PCR system using SYBR Green (Applied Biosystems Pte Ltd, Singapore). Primers used for RT-PCR are as follows: TAP1 forward, 5′-GGAGGCCTTGGCTTACGTCGC-3′; and reverse, 5′-GGAGCCCACAGCCTTCTGCA-3′; TAP2 forward, 5′-CCGGACCTGCCTTTCCTCATAGC-3′ and reverse, 5′-CCGCAGGTTGATCCTGGACATGG-3′; TAPASIN forward, 5′-CCAGCACTCTCTTCAGCCTCTCC-3′ and reverse, 5′-CCACTGTTGCCATGGTGATGAC-3′; GAPDH forward, 5'-CATCACTGCCACCCAGAAGACTG-3', reverse, 5'-ATGCCAGTGAGCTTCCCGTTCAG-3'. TRACP5 forward, 5'-GACCACAACCTGCAGTATCTT-3', and reverse, 5'-

GGGAGTCCTCAGATCCATAGT-3'; RPL12 forward, 5'-GGAAGGCATAGTGCTGGAGGT-3'; and reverse, 5'-CGATGACATCCTTGGCCTGA-3'.

1.4 Western Blotting

Following experimental treatment, cells were washed with ice-cold PBS, pelleted and re-suspended in RIPA lysis buffer (Sigma Aldrich, Singapore) supplemented with 1X complete protease inhibitor cocktail (Roche Ltd, Singapore). The supernatant was collected for SDS-PAGE analysis. Laemmli sample buffer (Bio-Rad, USA) was used to load proteins onto SDS PAGE gel. Equal amounts of protein from each sample were subjected to 15% SDS-PAGE at a constant voltage (125V) using mini-PROTEAN system (Bio-Rad Laboratories, Singapore). The proteins on SDS-PAGE gels were transferred onto Immun-Blot PVDF membrane (Bio-Rad, USA) using Trans-blot Turbo (Bio-Rad Laboratories, Singapore) according to manufacturer's protocol. Antibodies from Cell Signaling Technologies (USA) for western blot were: LysRS, MITF, Hint1, Histone H2A.X and α-tubulin. Ap_4A Hydrolase antibody was from Santa Cruz Biotechnology, USA.

For co-immunoprecipitation (pull down assay), Thermo Scientific Pierce IP lysis Buffer was used to extract proteins from cell lysate according to manufacturer's protocol, and was loaded onto SureBeads Protein G (Bio-Rad, USA) according to manufacturer's protocol. Briefly, 10 μg of LysRS antibody or 10 μg of IgG1 antibody (ThermoFisher Scientific, USA) was

added to 200 µl of SureBeads and the suspension was rotated for 10 mins at room temperature. The bead-antibody complex was then washed three times with 1 mL of PBS + 0.1% Tween 20 (PBS-T) by magnetization of beads to discard supernatant. 1 mg of protein lysate extracted using IP lysis buffer was added to the bead-antibody complex (per sample) and was rotated for 1 hr at room temperature. Beads were washed with 1 mL of PBS-T three times by magnetization. Laemmli sample buffer was used to load bead-antibody-protein complex onto 15% SDS-PAGE at a constant voltage (125V) using mini-PROTEAN system (Bio-Rad Laboratories, Singapore). The proteins on SDS-PAGE gels were transferred onto Immun-Blot PVDF membrane using Trans-blot Turbo (Bio-Rad Laboratories, Singapore) according to manufacturer's protocol. The resultant blot was probed with MITF antibody to detect MITF pull-down. Input lanes represent 5% of total protein lysate sample mixed with bead-antibody complex as a positive control.

1.5 Cell motility assay

To create a video recording of cells moving in a controlled environment, Olympus IX81 (Olympus, USA) inverted fluorescence microscope with stage-top live-cell imaging chamber with integrated 37˚C incubation chamber (model number TC-L-10. 96S106-O3, Chamlide, South Korea) maintained with 5.0% CO_2 for live capturing cells using a dynamically controlled heating stage that maintains the temperature during the time-lapse video recording (model number TC-L-10. 96S106-O3, Chamlide, South Korea).

MetaMorph NX (version 2.5) was used to capture the image and process for image analysis and post-processing of image was done with Fiji ImageJ (Schindelin *et al.*, 2012). To determine the motility of each cell, a specific position within the centre of nucleus using Manual Track plug-in for ImageJ (National Institute of Health, USA) analysis by frame-for-frame assigning tracker with tracer on an exact point in the nucleus over at least 20 frames was accomplished.

1.6 Generation of BMDCs

To generate BMDCs, the tibia and femur of mice were excised and the cells were suspended in RPMI containing 1% Hyclone Fetal Calf Serum (GE Healthcare, Singapore). After passing the cell suspension through 0.70 µm cell strainer (Thermo Fisher, Singapore) cells were pelleted (centrifugation at 300g for 7 min) and allowed for red blood cell lysis. The bone marrow cells were cultured at a concentration of 1 x 10^6 cells/ml in RPMI with 10% FCS, 1% non-essential amino acid (Sigma Aldrich), 1mM Sodium pyruvate (Sigma Aldrich), 5µM β-Mercaptoethanol (Sigma Aldrich), 100 IU/ml Penicillin (Sigma Aldrich), 0.1 mg/ml Streptomycin (Sigma Aldrich), and 5 ng/ml GM-CSF in 6-well plates. Cells were incubated in a humidified incubator at 37˚C, 5% CO_2. On day 2, 4 and 6, 75% of volume in medium was replaced with fresh medium supplemented with GM-CSF (5 ng/ml). After 7 days, the non- and loosely- adherent cells were harvested, washed, and magnetically isolated for CD11c positivity using anti-CD11c-conjugated MACS beads

(Miltenyl Biotec, USA). Flow-through or non-$CD11c^+$ cells were also collected as $CD11c^-$ cells as a control. The BMDCs were routinely examined and was $CD11c^+$ (high) MHC class II^+ (>90%).

1.7 Cell isolation

To isolate naïve $CD8^+$ T cells from OT-1 mice, spleens were collected from euthanized mice. Single-cell suspensions were layered on Ficoll-Paque (GE Healthcare, Singapore) and centrifuged at 600 *g* for 20 min. Cells accumulating at the interface were collected, washed twice with MACS buffer and incubated with anti-CD8α-conjugated magnetic cell sorting (MACS) beads (Miltenyi Biotec Pte Ltd, Singapore). Then the cells were isolated by passing through a MACS column. To isolate splenic DCs from *Nudt2*$^{fl/fl}$ mice and *Nudt2*$^{+/+}$ c57bl/6 mice spleens were perfused and digested with Liberase Cl (Roche) for 30 min at 37˚C. Single-cell suspensions were reconstituted with Optiprep (Sigma Aldrich) diluted to 1.062 g/ml and subjected to density centrifugation at 1700g, 10 min at 4˚C. Low-density cells that accumulated at the interface were collected, washed, and selected using anti-CD11c-conjugated MACS beads.

1.8 Small GTPase activity assay

The G-LISA small GTPase Activation Assay Biochemistry Combo Kit (RhoA, Rac1, cdc42) (Cytoskeleton, Colorado, USA) was used for the detection of

activated form of RhoA, Rac1 and cdc42 (i.e. GTP-bound form). The experiments were carried out in accordance to the manufacturer protocol.

1.9 FITC-dextran uptake assay

To measure the phagocytic ability of DCs, the cells were incubated with FITC-dextran (70,000 MW, Invitrogen, Singapore). The BMDCs cultured with GM-CSF for 8 days were seeded on 12-well plates at a concentration of 1.0×10^6 cells/well. FITC-dextran was added to a final concentration of 0.5 mg/ml. The cells were incubated in either 4˚C or 37˚C for 30 min. After the incubation period, the cells were detached from plate by flushing with media and collected (centrifugation at 500g for 5 min), followed by washing in excess 1% BSA/PBS. After giving twice washing cells were immediately subjected for FACS analysis and the median florescence intensity (MFI) for FITC was measured.

1.10 Co-culture for antigen cross-presentation to $CD8^+$ T cells

One µM of relevant peptide $OVA_{257–264}$ or whole OVA was added to DC (1 hr) and the excess unbound content was discarded. Subsequently, the OT-I $CD8^+$ T cells were co-cultured with peptide-pulsed DCs with or without LPS. Unless otherwise stated, cells were co-cultured in triplicate wells using U-bottomed 96-well plates with a total of 1×10^5 DCs / ml (100ul total volume) at a 10:1 $CD8^+$ T cell-to-DC ratio for 72 hr in a 37˚C/5% CO_2

incubator. CellTrace Violet (Invitrogen, USA) was used in accordance to manufacturer's protocol to label and measure proliferation of $CD8^+$ T cells.

1.11 Cytokine detection

The levels of IL-12p40 and IL-12p70 in culture supernatants were measured using the mouse DuoSet ELISA development kit (R&D Systems, USA) according to the manufacturer instructions. Analysis was performed using a Luminex 100 plate reader (Qiagen, USA).

1.12 Flow cytometry

After blocking the cells with anti-Fc antibody (anti-CD16/32; BD, United Kingdom), staining of cells was performed and are later re-suspended in flow buffer (PBS containing 2% BSA and 5mM EDTA). The following antibodies were purchased from (BD, USA), unless otherwise stated: anti-CD11c BV421, anti-CD8 APC, anti-CD80 PE, anti-CD86 APC, anti-CD40 Cy5.5 and anti-MHC class II (IA/IE) PB and a live/dead marker on APC-Cy7 (Invitrogen, USA). Cells were run on an LSR Fortessa or X-20 flow cytometer (BD, USA) and data were analysed by using the Flowjo analysis program (version 10.0.8).

1.13 Statistical analysis

The experimental significance between the treatments was calculated by performing analysis of variance (ANOVA) followed by Student's t test

Mann-Whitney test as appropriate (GraphPad Prism 7.01, USA). The experiments for which the *'P'* value <0.05 in comparison to the control were considered as statistically significant.

Supplemental References

- Murphy, G.A., Halliday, D., and McLennan, A.G. (2000). The Fhit Tumor Suppressor protein regulates the intracellular concentration of diadenosine triphosphate but not diadenosine tetraphosphate. Cancer Res. *60*, 2342 LP-2344.
- Schindelin, J., Arganda-Carreras, I., Frise, E., Kaynig, V., Longair, M., Pietzsch, T., Preibisch, S., Rueden, C., Saalfeld, S., Schmid, B., *et al.* (2012). Fiji: an open-source platform for biological-image analysis. Nat. Methods *9*, 676–682.